

## Investigation of some niobate-based dielectrics in view of base metal co-sintering

Sophie d'Astorg\*, Sylvain Marinel, Olivier Perez, Attila Veres

CRISMAT Laboratory, UMR6508 CNRS/ENSICAEN, 6 Bd Maréchal Juin 14050 Caen cedex, France

Received 15 October 2006; received in revised form 31 January 2007; accepted 18 February 2007

Available online 4 May 2007

### Abstract

Bearing in mind the excellent dielectric properties at high frequency of some niobates like  $\text{ZnNb}_2\text{O}_6$ ,  $\text{Zn}_3\text{Nb}_2\text{O}_8$ ,  $\text{BaNb}_2\text{O}_6$ ,  $\text{Ba}_5\text{Nb}_4\text{O}_{15}$  ( $\epsilon_r \sim 20\text{--}45$ ,  $\tan \delta < 10 \times 10^{-4}$  and  $\rho_i > 10^{10} \Omega \text{ cm}$ ), synthesis, sintering and properties of these oxides are reported. The lowering of their sintering temperature has been investigated for these four ceramics using sintering aids. Using appropriate additive, it is possible to densify these ceramics at a temperature for which base metal electrodes, *e.g.* Cu and Ag can be employed. Two formulations were found to be sinterable at  $1000^\circ\text{C}$  (lower than the copper melting point) whereas a third formulation is co-sinterable with silver electrodes. For this later, the dielectric properties are globally maintained in comparison with the pure compound sintered at  $1200^\circ\text{C}$ . This result makes this formulation suitable for silver based passive components devices manufacturing.

© 2007 Elsevier Ltd. All rights reserved.

**Keywords:** Sintering; Dielectric properties; Niobates; Capacitors;  $\text{ZnNb}_2\text{O}_6$ ;  $\text{BaNb}_2\text{O}_6$

### 1. Introduction

Investigations performed to design ceramics with low dielectric losses, high permittivity, high resistivity and low sintering temperature are the key to produce low cost–high performance passive components such as ceramic capacitors or hyperfrequency resonators. In this context, a large variety of ceramic structures have been explored like perovskites<sup>1–3</sup> or other derived structures.<sup>4</sup> These materials often exhibit interesting dielectric properties but also have very high sintering temperature (*i.e.*  $>1500^\circ\text{C}$ ) which is a real drawback to envisage a co-sintering with base metal (copper or silver). Among this family of interesting compounds, some materials having both a relative low sintering temperature ( $<1400^\circ\text{C}$ ) and attractive dielectric properties have been selected:  $\text{Ba}_5\text{Nb}_4\text{O}_{15}$ ,  $\text{BaNb}_2\text{O}_6$ ,  $\text{ZnNb}_2\text{O}_6$  and  $\text{Zn}_3\text{Nb}_2\text{O}_8$ .

Galasso and Katz<sup>5</sup> described the  $\text{Ba}_5\text{Nb}_4\text{O}_{15}$  structure as a five  $\text{BaO}_3$  layers in which niobium ions are in octahedral coordination with oxygen. The dielectric data for this compound were first reported by Sreemoolanadhan *et al.*<sup>6</sup> They measured,

using a cavity method, a Q.f factor of around 12,700 GHz, a room temperature relative permittivity of 38.4 and a temperature coefficient of the resonant frequency of  $-9 \text{ ppm } ^\circ\text{C}^{-1}$ . One year later, Vineis and Davies reported a Q.f factor of 26,337 GHz at 8.59 GHz, a relative dielectric constant  $\epsilon_r$  of 39.3 and a temperature coefficient of resonant frequency  $\tau_f$  of  $79.1 \text{ ppm } ^\circ\text{C}^{-1}$ .<sup>7</sup> Other papers report similar values to Vineis and Davies's results.<sup>8,9</sup> More recently, Ratheesh *et al.* used the whispering gallery mode technique to characterize the microwave dielectric properties of  $\text{Ba}_5\text{Nb}_4\text{O}_{15}$  and found Q.f = 53,000 GHz at 16 GHz,  $\epsilon_r = 40$ ,  $\tau_f = 78 \text{ ppm } ^\circ\text{C}^{-1}$ .<sup>10</sup> These characterizations have been done using microwave techniques and the relative disparity of the results could be explained by some differences in term of sample's synthesis reflected in microstructure, density, grains size, purity, etc.

The  $\text{BaNb}_2\text{O}_6$  compound may exist as two polymorphs, one is a good resonator with a Q.f factor of 43,000 GHz,  $\epsilon_r$  of 30 and  $\tau_f$  of  $-45 \text{ ppm } ^\circ\text{C}^{-1}$ .<sup>11</sup> This polymorph is orthorhombic and stable at high temperatures (above  $1150^\circ\text{C}$ ). The second polymorph, stable below  $1150^\circ\text{C}$ , has a hexagonal structure and exhibits a Q.f factor of 4000 GHz,  $\epsilon_r$  of 42 and  $\tau_f$  of  $-800 \text{ ppm } ^\circ\text{C}^{-1}$ . It is also pointed out that the hexagonal phase is ferroelectric up to  $1050^\circ\text{C}$ . The full densification of the hexagonal  $\text{BaNb}_2\text{O}_6$  compound is reported to be difficult due to the

\* Corresponding author.

E-mail address: [sophie.d.astorg@ensicaen.fr](mailto:sophie.d.astorg@ensicaen.fr) (S. d'Astorg).

orthorhombic-hexagonal phase transition which occurs during the cooling from the high temperature stage. To avoid this critical transition, for the densification, one method consists in using a hot pressing sintering process in order to obtain dense  $\text{BaNb}_2\text{O}_6$  compound at around  $1050^\circ\text{C}$ .

The dielectric properties of  $\text{ZnNb}_2\text{O}_6$  were investigated by Maeda et al.<sup>12</sup> They reported that  $\text{ZnNb}_2\text{O}_6$  exhibits a large Q.f value (44,000 at 4 GHz) and a relative permittivity of 20. Later, Lee et al. obtained a higher Q.f factor (Q.f = 83,700 at 10 GHz,  $\epsilon_r = 25$  and  $\tau_f = -56.1 \text{ ppm } ^\circ\text{C}^{-1}$ )<sup>13</sup> and Pullar et al. have confirmed these attractive properties (Q.f = 84,500 at 6.29 GHz,  $\epsilon_r = 23.2$  and  $\tau_f = -75.8 \text{ ppm } ^\circ\text{C}^{-1}$ ).<sup>14</sup>

Recently  $\text{Zn}_3\text{Nb}_2\text{O}_8$  compound has emerged as a good microwave material thanks to its high quality factor higher than 80,000 GHz, its relative permittivity of 21.6 and its temperature coefficient of resonant frequency  $\tau_f$  of  $-71 \text{ ppm } ^\circ\text{C}^{-1}$ .<sup>15</sup>

The literature is rich in microwave characterization of niobates for resonators application. Most of these oxides showing high Q.f factor and a permittivity varying from 20 to 40, lead possible the use of them as type I dielectric to produce base metal multi-layer capacitors using copper or silver as electrodes in high frequency range (MHz). Nevertheless, there is a lack of information concerning this specific application. The purpose of our work is to investigate the lowering of the sintering temperature of these niobates using conventional sintering aids like  $\text{V}_2\text{O}_5$ ,  $\text{SiO}_2$ ,  $\text{B}_2\text{O}_3$ . Even if some studies have already reported the effects of some additives on the sintering temperature lowering of  $\text{Ba}_5\text{Nb}_4\text{O}_{15}$ <sup>16</sup> or  $\text{Zn}_3\text{Nb}_2\text{O}_8$ ,<sup>15,17</sup> none systematically study has been focused on this point. This paper will describe for the four selected niobates, the synthesis, the sintering with and without additives, the microstructure as well as the dielectric properties. Some co-sintered prototypes based on copper or silver were also designed and characterized.

## 2. Experimental procedure

The four compounds,  $\text{Ba}_5\text{Nb}_4\text{O}_{15}$ ,  $\text{BaNb}_2\text{O}_6$ ,  $\text{ZnNb}_2\text{O}_6$ , and  $\text{Zn}_3\text{Nb}_2\text{O}_8$  have been synthesised. For brevity, these four compounds are named by a number XYZ defined as follows  $\text{Ba}_x\text{Zn}_y\text{Nb}_z\text{O}_{0.5(2x+2y+5z)}$ . Then  $\text{Ba}_5\text{Nb}_4\text{O}_{15}$  is named as 504,  $\text{BaNb}_2\text{O}_6$  as 102,  $\text{ZnNb}_2\text{O}_6$  as 012 and  $\text{Zn}_3\text{Nb}_2\text{O}_8$  as 032. The 504, 102, 012 and 032 phases have been obtained by solid-state reaction. For the present purpose,  $\text{BaCO}_3$  (Diopma, 99.99%),  $\text{ZnO}$  (Cerac, 99.995%), and  $\text{Nb}_2\text{O}_5$  (HCS Starck, 99.9%) powders were mixed in appropriate proportions and mechanically grinded in a Teflon jar by using zircon balls (1 mm in diameter) for 2 h in ammoniac solution. The resulting slurry was subsequently dried under infra-red lamps and manually regrinded. The 504, 102 and 032 resulting powders were heat treated at  $1100^\circ\text{C}$  and the 012 at  $1000^\circ\text{C}$  in air for 2 h with a heating and cooling rate of  $200^\circ\text{C h}^{-1}$ . The resulting compounds were again grinded in a teflon jar for 1 h using the same process, then powders were dried and manually grinded. Sintering additives ( $\text{B}_2\text{O}_3$  (Cerac, 99.9%),  $\text{SiO}_2$  (ICN, >99%),  $\text{V}_2\text{O}_5$  (Rectapur, 99.5%)) were manually mixed with the dielectric compound in an agate mortar, with a 10 mol% ratio. Cylindrical pellets were shaped, having suitable dimensions, by

employing a uni-axial pressure of 1.5 MPa. Sintering temperatures were systematically determined by thermo-mechanical analysis (SETARAM TMA 92). X-ray diffraction studies were performed using a Rigaku X-ray diffractometer equipped with  $\text{Cu K}\alpha$  radiation. Full pattern matching analysis of the different XRD patterns were performed using the Jana2000 software; the cell parameters were then extracted for all samples and the secondary phases were identified.<sup>18</sup> The microstructure was examined by a Philips scanning electron microscope (model no. Feg XI'30). The dielectric measurements at 1 MHz were carried out as a function of temperature in the range of  $-60$  to  $160^\circ\text{C}$ , using a Flucke LCR Bridge (model no. PM6306). The resistivity was measured using a SEFELEC DM500A megohmmeter. Copper ink (TANAKA C4118) as well as silver paste (Dupont) was used to fabricate co-sintered prototypes. Metallic ink was manually deposited on each face of dielectric disks for electrodes. For copper co-sintering, a flow of  $\text{Ar}/\text{H}_2$  10% gas was used to avoid electrodes oxidation whereas silver co-sintering was performed in ambient.

## 3. Results and discussion

### 3.1. Pure materials

XRD patterns show that all pure compounds are single phase (Fig. 1). The unit cell parameters of 504 has been refined taking into account a space group  $P-3m1$  with hexagonal structure and the cell parameters are  $a = 5.7950(1) \text{ \AA}$  and  $c = 11.7851(3) \text{ \AA}$ . The 102 phase has a monoclinic structure with the space group  $P21/c$  and cell parameters are  $a = 3.9480(3) \text{ \AA}$ ,  $b = 6.0458(4) \text{ \AA}$ ,  $c = 10.4290(7) \text{ \AA}$ ,  $\alpha = \gamma = 90^\circ$  and  $\beta = 90.356(4)^\circ$ . The 032 phase crystallises in the monoclinic structure with the space group  $C2/c$  and the cell parameters are  $a = 19.0175(7) \text{ \AA}$ ,  $b = 5.9032(2) \text{ \AA}$ ,  $c = 5.1957(2) \text{ \AA}$  and  $\beta = 90.093(5)^\circ$ . Finally, the 012 phase has an orthorhombic structure, space group  $Pbcn$ , and lattice cell parameters are  $a = 14.1768(4) \text{ \AA}$ ,  $b = 5.7178(2) \text{ \AA}$  and  $c = 5.0288(1) \text{ \AA}$ .

Thermodilatometric analysis was performed on each pure compound and results are shown in Fig. 2. From the dilatometric curves, it is clearly evidenced that all pure compounds require a temperature close to  $1200^\circ\text{C}$  to achieve a satisfying density. All compositions were subsequently sintered at this temperature in air, during 2 h in order to have a set of references. All ceramics exhibit very good densities (>90% of the theoretical one) which are close to their theoretical value and the dielectric properties of these compounds are given Table 1. One can clearly evidence that the experimental values of  $\epsilon_r$  are in good agreement with previous published results for all investigated materials. The experimental  $\epsilon_r$  values of 504, 102, 012 and 032 are respectively 42.2, 42.2, 22.2 and 22.8 for 39, 42, 25 and 22 reported in the literature.<sup>6–10,11,13,15</sup> Moreover, all pure materials exhibit high value of insulating resistivity ( $>10^{11.5} \Omega \text{ cm}$ ) and low dielectrics losses ( $<10^{-3}$ ) that confirms the interest for these materials. Although main characteristics are attractive, these compounds exhibit also high temperature coefficients ( $\tau_f$  and  $\tau_\epsilon$ ). Nevertheless, this point is not really detrimental due to various temperature coefficient tuning methods, such as mix-

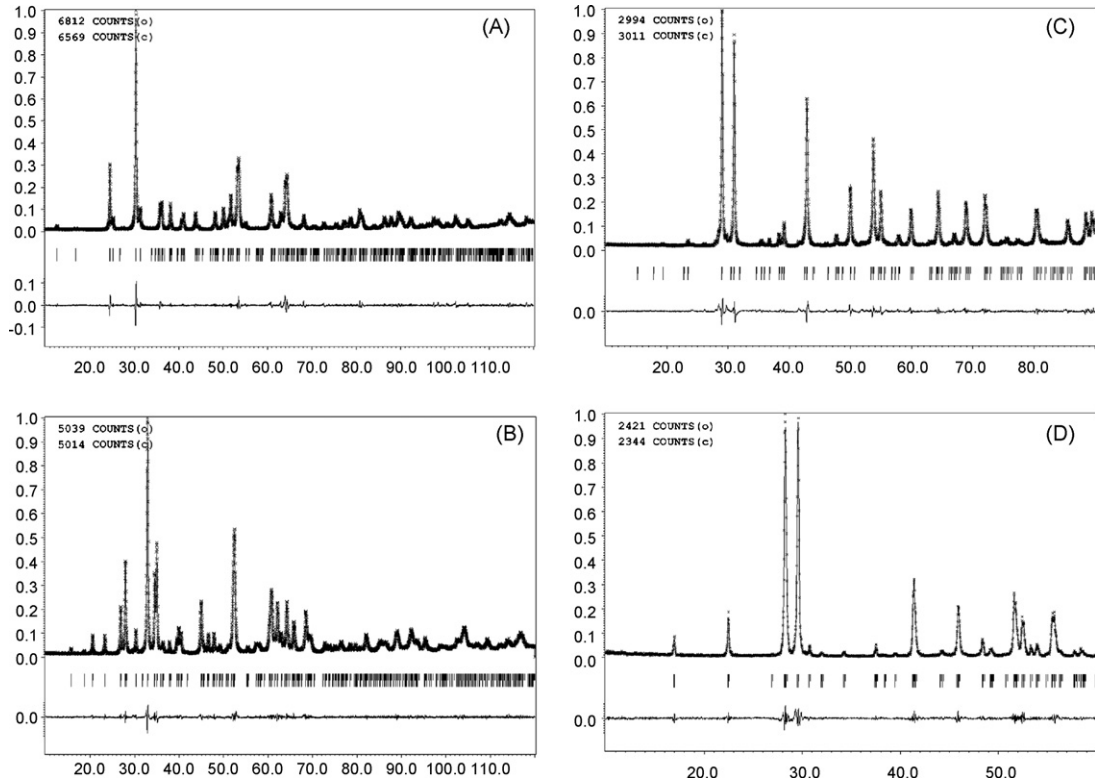


Fig. 1. Cu K $\alpha$  XRD patterns of (A) ZnNb<sub>2</sub>O<sub>6</sub>, (B) Zn<sub>3</sub>Nb<sub>2</sub>O<sub>8</sub>, (C) Ba<sub>5</sub>Nb<sub>4</sub>O<sub>15</sub> and (D) BaNb<sub>2</sub>O<sub>6</sub> in arbitrary unit vs.  $2\theta$  (°).

ing some dielectrics having opposite temperature coefficients, as Kim et al. did.<sup>19</sup>

Hyperfrequencies characteristics usually given in the literature are the temperature coefficient of the resonance frequency  $\tau_f$  and the Q.f product. The value of  $\tan(\delta)$  as well as the tem-

perature coefficient of the permittivity have capital importance for applications like multi-layer capacitors that justify our measurement of these characteristics. Nevertheless, it must be kept in mind that  $\tau_f$  is related to the thermal expansion coefficient,  $\alpha$ , and the temperature coefficient of permittivity,  $\tau_\epsilon$ , as follows:

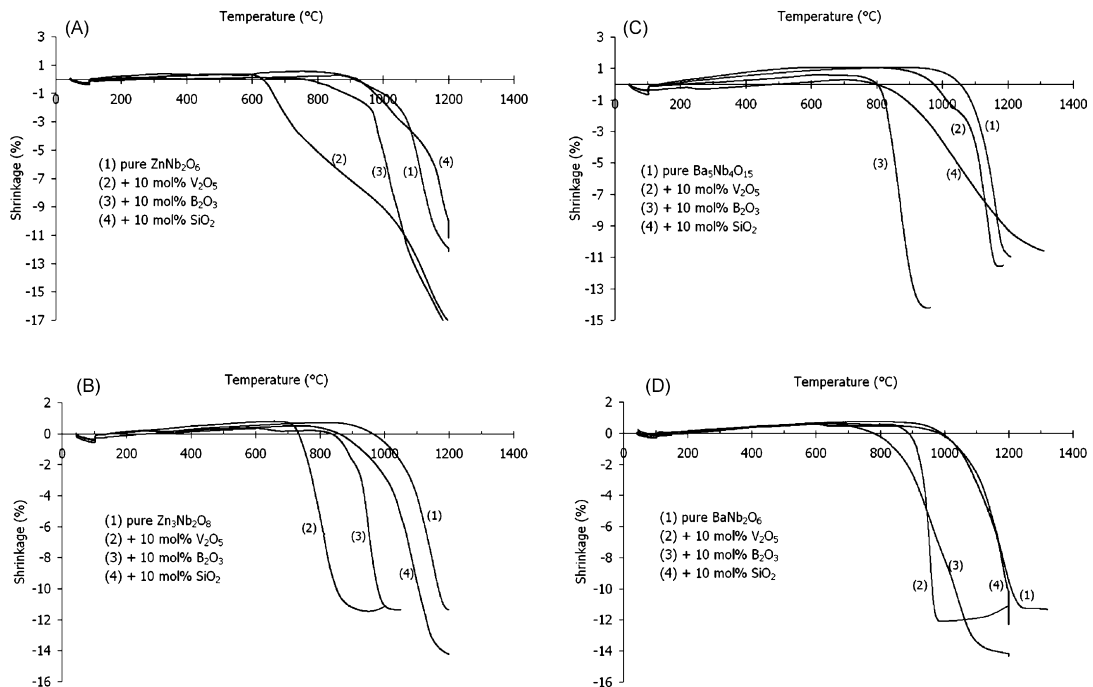


Fig. 2. Dilatometric curves of the pure niobates and of the sintering aids added materials.

Table 1  
Characteristics of pure compounds measured on disks, sintered at 1200 °C for 2 h in air and temperature coefficient of the resonant frequency extracted from literature

Compounds	Density (% of the theoretical)	tan( $\delta$ ) at 1 MHz ( $\times 10^{-4}$ )	$\epsilon_r$ (RT) at 1MHz	log( $\rho$ [ $\Omega$ cm])	$\tau_\epsilon$ (ppm/°C)	Corresponding $\tau_f$ (ppm/°C)	Published $\tau_f$ (ppm/°C)
Ba <sub>5</sub> Nb <sub>4</sub> O <sub>15</sub>	>90%	<10	42.2	11.5	−171	75.5	79.1 <sup>7</sup>
BaNb <sub>2</sub> O <sub>6</sub>	>92%	<10	42.2	11	+330	−175	−800 <sup>11</sup>
ZnNb <sub>2</sub> O <sub>6</sub>	>92%	<10	22.2	12.5	197	−108.5	−75.8 <sup>14</sup>
Zn <sub>3</sub> Nb <sub>2</sub> O <sub>8</sub>	>94%	<10	22.8	11.4	217	−118.5	−71 <sup>15</sup>

$\tau_f = -\alpha - (1/2)\tau_\epsilon$ . Since  $\alpha$  of microwave niobates is known to be in range of 10 ppm °C<sup>−1</sup>,<sup>13</sup>  $\tau_f$  depends on  $\tau_\epsilon$  and vice versa. A  $\tau_\epsilon$  value of −20 ppm °C<sup>−1</sup> should permit to obtain  $\tau_f$  close to zero. Considering that the thermal expansion coefficient  $\alpha$  value is in range of 10 ppm °C<sup>−1</sup>, the  $\tau_f$  coefficient has been calculated from the experimental  $\tau_\epsilon$  values (Table 1). For the 5 0 4 compound, the calculated value of  $\tau_f = 75.5$  ppm °C<sup>−1</sup> is in good agreement in respect to 79.1 ppm °C<sup>−1</sup> value, published in literature.<sup>7</sup> The agreement between calculated and published results for  $\tau_f$  is less satisfying for 0 1 2 and 0 3 2 compounds but the same order of value is obtained (Table 1). For the 1 0 2 phase, a large difference is observed since calculated value of  $\tau_f$  is −175 ppm °C<sup>−1</sup> whereas the value extracted from literature is −800 ppm °C<sup>−1</sup>. An explanation is that this compound exists as two polymorphs: the orthorhombic phase exhibits a  $\tau_f$  value of −45 ppm °C<sup>−1</sup> and the hexagonal −800 ppm °C<sup>−1</sup>. BaNb<sub>2</sub>O<sub>6</sub> has been sintered at 1200 °C and multiphase material has been probably obtained during the sintering step.<sup>11</sup> Nevertheless, this discussion should be carefully considered since the  $\tau_f$  value is estimated from  $\tau_\epsilon$  measurement at MHz whereas the  $\tau_f$  value, extracted from the literature, has been measured at GHz.

### 3.2. Sintering aids added materials

Three oxides B<sub>2</sub>O<sub>3</sub>, SiO<sub>2</sub>, V<sub>2</sub>O<sub>5</sub> have been added as flux to decrease the sintering temperature. Our study shows the beneficial effect of V<sub>2</sub>O<sub>5</sub> and B<sub>2</sub>O<sub>3</sub> as sintering additives on the sintering temperature lowering for the 1 0 2, 5 0 4 and 0 3 2 compounds (Fig. 2). Hence, according to the thermo-mechanical analysis, it is possible to co-sinter 0 3 2 + V<sub>2</sub>O<sub>5</sub> as well as 5 0 4 + B<sub>2</sub>O<sub>3</sub> ceramics with silver whereas the compositions 0 3 2 + B<sub>2</sub>O<sub>3</sub> and 1 0 2 + V<sub>2</sub>O<sub>5</sub> could be compatible with a copper co-sintering. Table 2 summarizes the shrinkage achievement temperature for these four formulations. It must be noticed that this co-sinterability was deduced only from the densification temperature. Consequently, these latter compositions were subsequently selected to test the co-sintering process. For the co-sintered material properties investigation, each face of 0 3 2 + V<sub>2</sub>O<sub>5</sub> and 5 0 4 + B<sub>2</sub>O<sub>3</sub> disks was manually covered by

silver paste whereas disks of 0 3 2 + B<sub>2</sub>O<sub>3</sub> and 1 0 2 + V<sub>2</sub>O<sub>5</sub> were covered by copper ink. The sintering conditions used for their densification are summarized Table 2.

### 3.3. Silver co-sintered prototypes

SEM images of the co-sintered prototypes are shown in Fig. 3. High magnification microstructures of 5 0 4 (Fig. 3A) and 0 3 2 (Fig. 3B) show a satisfying density.

For the 5 0 4 compound, the interface between the silver layers and the ceramic is very sharp and no diffusion of silver in the ceramic is observed, as examined by the EDS silver profile analysis. One co-sintered pellet was also manually crushed and X-ray diagram was recorded on it (Fig. 4A). The refinement of the lattice parameters of the 5 0 4 phase in both cases gives quite similar results ( $a = 5.7954(1)$  Å and  $c = 11.7921(2)$  Å when B<sub>2</sub>O<sub>3</sub> is added compared to  $a = 5.7950(1)$  Å and  $c = 11.7851(3)$  Å for the B<sub>2</sub>O<sub>3</sub> free one). The main observable difference is that with B<sub>2</sub>O<sub>3</sub> addition, a very slight peak in the diffraction pattern appears at  $2\theta = 29.63^\circ$  (see the narrow on the XRD diagram). This peak could be the sign of the presence of traces of BaNb<sub>2</sub>O<sub>6</sub>. This result has been already reported by Kim et al.<sup>16</sup> when B<sub>2</sub>O<sub>3</sub> was added to the 5 0 4 phase. As the ceramic is not significantly altered by the B<sub>2</sub>O<sub>3</sub> addition, no degradation of the dielectric properties is expected. Our measurements account for this (Fig. 5): the observed dielectric constant ( $\epsilon_r$ ) of silver/5 0 4 + B<sub>2</sub>O<sub>3</sub> compound is 37, the dielectric losses are low ( $\sim 10^{-3}$ ) and the resistivity is around  $10^{11}$  Ω cm. Furthermore, the temperature dependence of the dielectric constant is linear and the extracted value of the permittivity temperature coefficient is −150 ppm °C<sup>−1</sup>, which is in good agreement with the value obtained for the pure compound, *i.e.*, −171 ppm °C<sup>−1</sup>. In the case of the 0 3 2 + V<sub>2</sub>O<sub>5</sub> compound, diffusion of Ag in the ceramic was observed (Fig. 3B). Most likely, as the co-sintering temperature (900 °C) is far from the silver melting point (961 °C) and according to the study of the vanadium pentoxide silver system by Volkov et al.<sup>20</sup> an eutectic type reaction between the electrodes and the ceramic could explain this phenomena. It is also an explana-

Table 2  
Co-sintering conditions

Composition	Sintering temperature (°C)	Test Ag co-sintering	Test Cu co-sintering
5 0 4 + B <sub>2</sub> O <sub>3</sub>	950	950 °C–2 h air ± 200 °C/h	
0 3 2 + V <sub>2</sub> O <sub>5</sub>	900	900 °C–2 h air ± 200 °C/h	
1 0 2 + V <sub>2</sub> O <sub>5</sub>	1000		1000 °C–2 h Ar/H <sub>2</sub> (10%) ± 200 °C/h
0 3 2 + B <sub>2</sub> O <sub>3</sub>	1000		1000 °C–2 h Ar/H <sub>2</sub> (10%) ± 200 °C/h

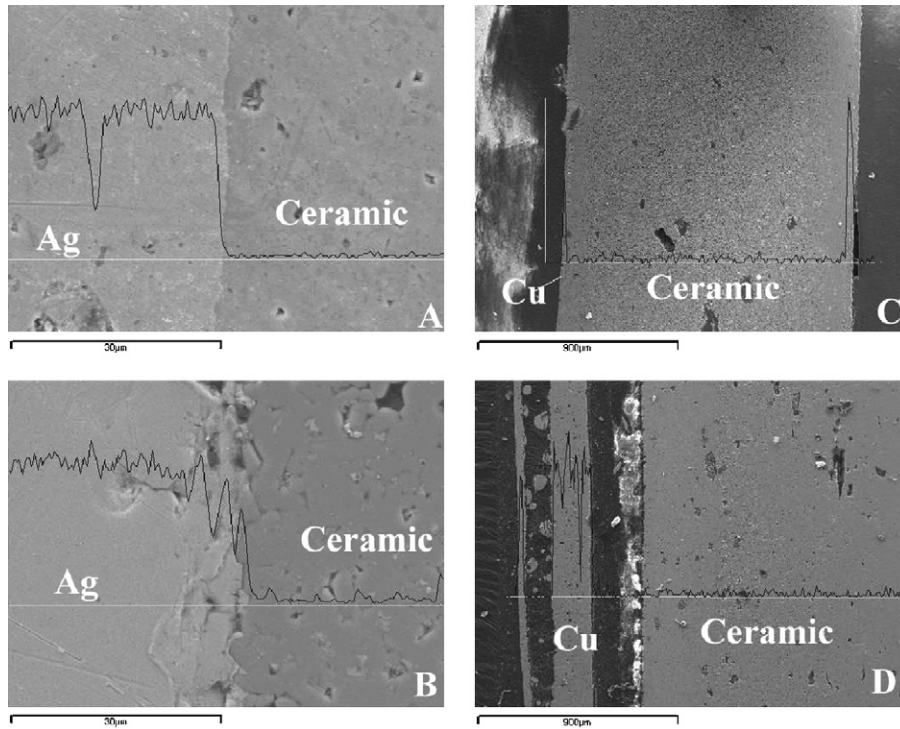


Fig. 3. SEM microstructure of co-sintered prototypes: (A) 504 + B<sub>2</sub>O<sub>3</sub>/Ag, (B) 032 + V<sub>2</sub>O<sub>5</sub>/Ag, (C) 032 + B<sub>2</sub>O<sub>3</sub>/Cu and (D) 102 + V<sub>2</sub>O<sub>5</sub>/Cu.

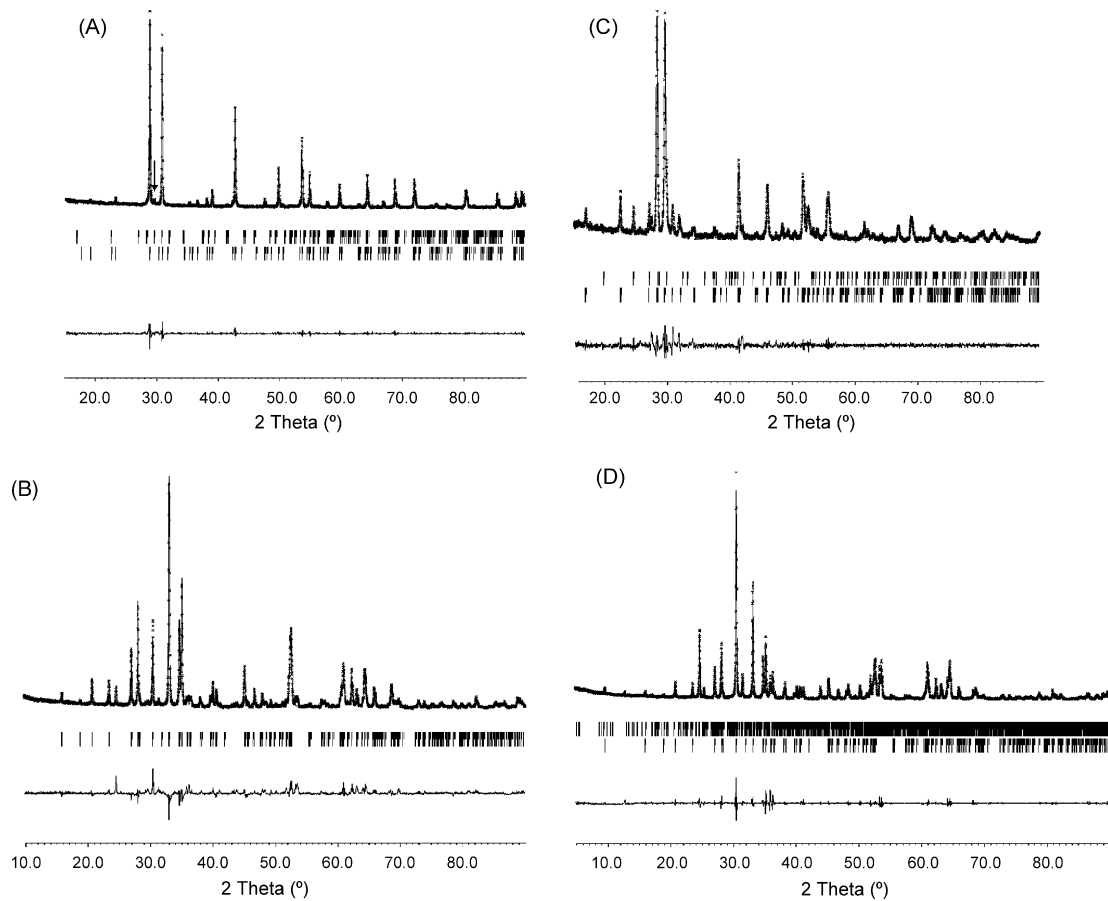


Fig. 4. XRD pattern of the four co-sintered pellets in arbitrary unit versus  $2\theta$  (°): (A) 504 + B<sub>2</sub>O<sub>3</sub>, (B) 032 + V<sub>2</sub>O<sub>5</sub>, (C) 032 + B<sub>2</sub>O<sub>3</sub> and (D) 102 + V<sub>2</sub>O<sub>5</sub>.

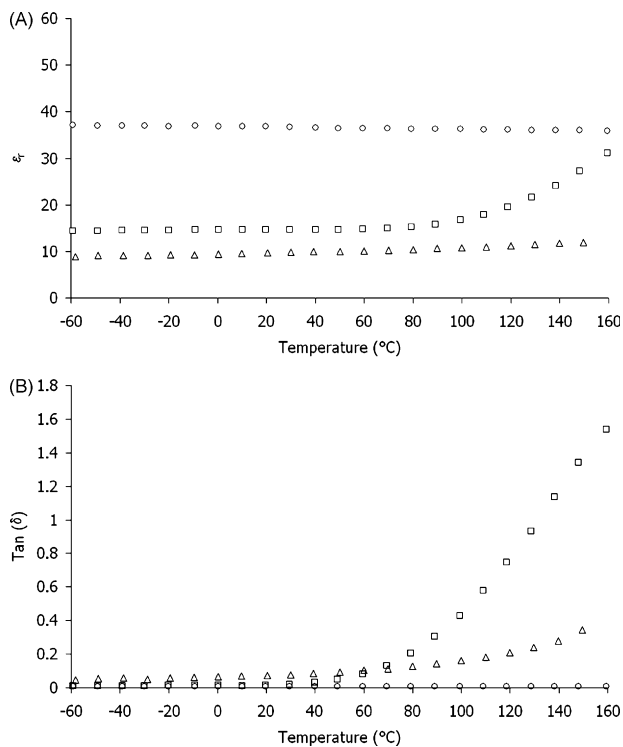


Fig. 5. Characteristics (relative permittivity (A) and losses factor (B)) of co-sintered disks: 5.04 + B<sub>2</sub>O<sub>3</sub>/Ag (○), 0.32 + B<sub>2</sub>O<sub>3</sub>/Cu (□), 1.02 + V<sub>2</sub>O<sub>5</sub> (△), measured at 1 MHz, vs. temperature.

tion for the bad dielectric properties of this sample (Fig. 5). The XRD pattern of the co-sintered prototype (Fig. 4B), performed after crushing the sintered sample, does not reveal a significant modification of the cell parameters ( $a = 18.9994(7) \text{ \AA}$ ,  $b = 5.9018(2) \text{ \AA}$ ,  $c = 5.1895(2) \text{ \AA}$  and  $\beta = 90.109(3)^\circ$ ). Nevertheless, a small amount of Nb<sub>2</sub>O<sub>5</sub> was identified in the diffraction pattern. Since the corresponding diffraction peaks were not overlapped by other peaks, it has been possible to perform a Rietveld analysis. The structure of Zn<sub>3</sub>Nb<sub>2</sub>O<sub>8</sub> has been thus introduced. The atomic positions as well as the cationic site occupation were refined and the obtained reliability factors are satisfying ( $R_p = 8.96\%$ ,  $R_{obs} = 7.34\%$ ). The niobium site occupancy was found to be lower than the unit suggesting for this site, the presence of both niobium and a specie with a lower atomic number as vanadium. This refinement leads to the fact that vanadium can substitute for niobium rejecting it from the structure. Such V/Nb substitution has already been observed in the case of ZnNb<sub>2</sub>O<sub>6</sub>.<sup>21</sup>

### 3.4. Copper co-sintered prototypes

Structural details and properties studies were also carried out with Cu-based electrodes materials. Fig. 3C shows microstructure of compound 0.32 + B<sub>2</sub>O<sub>3</sub> co-sintered with copper at 1000 °C in Ar/H<sub>2</sub> mixture gas. SEM image reveals a well dense microstructure. Furthermore, the detail EDS analysis clearly shows that there is no diffusion of copper into the bulk matrix. Dielectric properties versus temperature for this prototype are shown in Fig. 5. The dielectric behaviour is nearly constant

up to 60 °C, but from this value, dielectric permittivity as the losses factor monotonously increases with temperature. This may be due to the increase in their conductivity since the reducing atmosphere has probably induced a partial reduction/decomposition of the 0.32 oxide. The relatively high weight losses (around 17%) during the sintering stage actually accounts for the volatilization of ZnO. This was confirmed by the XRD pattern performed on the Cu co-sintered prototype which shows the presence of Zn<sub>3</sub>Nb<sub>2</sub>O<sub>8</sub> and Nb<sub>2</sub>O<sub>5</sub> (Fig. 4C). This phenomenon is well known in some Zn-based compounds sintered in Ar/H<sub>2</sub> atmosphere.<sup>22</sup> Finally, the full pattern matching analysis leads to the following cell parameters  $a = 19.0111(5) \text{ \AA}$ ,  $b = 5.9049(2) \text{ \AA}$  and  $c = 5.19035(2) \text{ \AA}$  and  $\beta = 90.123(3)^\circ$  for Zn<sub>3</sub>Nb<sub>2</sub>O<sub>8</sub>.

The Cu/1.02 + 10 mol% V<sub>2</sub>O<sub>5</sub> compound was sintered at 1000 °C and studied too. Its microstructure and compositional analysis are shown in Fig. 3D. The ceramic is well dense. However, a problem of delaminating appears at the ceramic/metal interface, which may be due to their shrinkage difference. As a consequence, it induces the presence of air gap between the two electrodes, which clearly explains the observation of low dielectric constant ( $\epsilon_r \sim 9.7$ ) in this system, which is two times lower than the bulk value. The XRD pattern of the co-sintered sample shows the existence of secondary phases like Nb<sub>2</sub>O<sub>5</sub> among others (Fig. 4D). However, the presence of these secondary phases prevents satisfying Rietveld analysis and thus a possible Nb for V substitution cannot be evidenced.

## 4. Conclusion

The ZnNb<sub>2</sub>O<sub>6</sub>, Zn<sub>3</sub>Nb<sub>2</sub>O<sub>8</sub>, BaNb<sub>2</sub>O<sub>6</sub>, Ba<sub>5</sub>Nb<sub>4</sub>O<sub>15</sub> niobates have been successfully synthesised as single phases. Effects of the various additives, B<sub>2</sub>O<sub>3</sub>, SiO<sub>2</sub>, V<sub>2</sub>O<sub>5</sub>, on the structure and properties of these compounds have been investigated. Employing suitable additives, it is possible to lower the sintering temperature at a level where Cu or Ag electrodes can be employed. The B<sub>2</sub>O<sub>3</sub> and V<sub>2</sub>O<sub>5</sub> additions are the most effective and allow to sinter Ba<sub>5</sub>Nb<sub>4</sub>O<sub>15</sub>, BaNb<sub>2</sub>O<sub>6</sub> and Zn<sub>3</sub>Nb<sub>2</sub>O<sub>8</sub> at reduced temperatures: 950 °C for Ba<sub>5</sub>Nb<sub>4</sub>O<sub>15</sub> with 10 mol% B<sub>2</sub>O<sub>3</sub>, 900 °C for Zn<sub>3</sub>Nb<sub>2</sub>O<sub>8</sub> with 10 mol% V<sub>2</sub>O<sub>5</sub>, 1000 °C for BaNb<sub>2</sub>O<sub>6</sub> with 10 mol% V<sub>2</sub>O<sub>5</sub> and Zn<sub>3</sub>Nb<sub>2</sub>O<sub>8</sub> with 10 mol% B<sub>2</sub>O<sub>3</sub>. Two types of co-sintered compounds were designed: the first two compounds with silver and the last two with copper in Ar/H<sub>2</sub> atmosphere.

The two copper co-sintered disks exhibit low relative permittivities, and instability of their dielectric properties versus temperature. Such behaviours were supposed to be due to the decomposition of the oxide during sintering in reductive atmosphere.

In the case of Zn<sub>3</sub>Nb<sub>2</sub>O<sub>8</sub> + 10 mol% V<sub>2</sub>O<sub>5</sub>/Ag, the negative effect of an eutectic, between silver and V<sub>2</sub>O<sub>5</sub>, on the physical properties was clearly observed. For this formulation it was also evidenced that vanadium can enter into the structure in the niobium sites.

The Ba<sub>5</sub>Nb<sub>4</sub>O<sub>15</sub> + 10 mol% B<sub>2</sub>O<sub>3</sub>/Ag is the most interesting formulation for several reasons: its relative permittivity ( $\epsilon_r = 37$  at RT), its stability versus temperature ( $\tau_f \sim +65 \text{ ppm } ^\circ\text{C}^{-1}$ ),

its low dielectric losses ( $\tan(\delta) < 10^{-3}$ ) and its co-sinterability with silver.

## References

1. Setter, N. and Waser, R., Electroceramic materials. *Acta Mater.*, 2000, **48**, 151–178.
2. Wersing, W., Microwave ceramics for resonators and filters. *Curr. Opin. Solid State Mater. Sci.*, 1996, **1**(5), 715–731.
3. Kawashima, S., Nishida, M., Ueda, I. and Oushi, H.,  $\text{Ba}(\text{Zn}_{1/3}\text{Ta}_{2/3})\text{O}_3$  ceramics with low dielectric loss at microwave frequencies. *J. Am. Ceram. Soc.*, 1983, **66**(6), 421–423.
4. Marinell, S. and Roulland, F., Synthesis and characterisation of the double perovskite  $\text{Ba}_2(\text{Zn}_{0.5}\text{Ti}_{0.5}\text{X})\text{O}_6$  ( $\text{X}=\text{Nb}$ ,  $\text{Ta}$ ) ceramics. *Mater. Res. Bull.*, 2005, **40**, 962–969.
5. Galasso, F. and Katz, L., Preparation and structure of  $\text{Ba}_5\text{Ta}_4\text{O}_{15}$  and related compounds. *Acta Crystallogr.*, 1961, **14**, 647–650.
6. Sreemoolanadhan, H. and Sebastian, M. T., High permittivity and low loss ceramics in the  $\text{BaO}-\text{SrO}-\text{Nb}_2\text{O}_5$  system. *Mater. Res. Bull.*, 1995, **30**(6), 653–658.
7. Vineis, C. and Davies, P. K., Microwave dielectric properties of hexagonal perovskites. *Mater. Res. Bull.*, 1996, **31**(5), 431–437.
8. Jawahar, I. N., Mohanan, P. and Sebastian, M. T.,  $\text{A}_5\text{B}_4\text{O}_{15}$  ( $\text{A}=\text{Ba}$ ,  $\text{Sr}$ ,  $\text{Mg}$ ,  $\text{Ca}$ ,  $\text{Zn}$ ;  $\text{B}=\text{Nb}$ ,  $\text{Ta}$ ) microwave dielectric ceramics. *Mater. Lett.*, 2003, **57**, 4043–4048.
9. Kamba, S., Petzelt, J., Buixaderas, E., Haubrich, D. and Vanek, P., High frequency dielectric properties of  $\text{A}_5\text{B}_4\text{O}_{15}$  microwave ceramics. *J. Appl. Phys.*, 2001, **89**(7), 3900–3906.
10. Ratheesh, R., Sebastian, M. T., Mohanan, P., Tobar, M. E., Hartnett, J., Woode, R. et al., Microwave characterisation of  $\text{BaCe}_2\text{Ti}_5\text{O}_{15}$  and  $\text{Ba}_5\text{Nb}_4\text{O}_{15}$  ceramic dielectric resonators using whispering gallery mode method. *Mater. Lett.*, 2000, **45**, 279–285.
11. Kim, D.-W., Hong, H. B., Hong, K. S., Kim, C. K. and Kim, D. J., The reversible phase transition and dielectric properties of  $\text{BaNb}_2\text{O}_6$  polymorphs. *Jpn. J. Appl. Phys.*, 2002, **41**, 6045–6048.
12. Maeda, M., Yamamura, T. and Ikeda, T., Dielectric characteristics of several complex oxide ceramics at microwaves frequencies. *Jpn. J. Appl. Phys.*, 1987, **26**(2), 76–79.
13. Lee, H.-J., Hong, K.-S. and Kim, S.-J., Dielectric properties of  $\text{MNB}_2\text{O}_6$  compounds (where  $\text{M}=\text{Ca}$ ,  $\text{Mn}$ ,  $\text{Co}$ ,  $\text{Ni}$  or  $\text{Zn}$ ). *Mater. Res. Bull.*, 1997, **32**(7), 847–855.
14. Pullar, R. C., Breeze, J. D. and Alford, N. McN., Characterization and microwave dielectric properties of  $\text{M}^{2+}\text{Nb}_2\text{O}_6$ . *J. Am. Ceram. Soc.*, 2005, **88**(9), 2466–2471.
15. Kim, D.-W., Kim, J.-H., Kim, J.-R. and Hong, K.-S., Phase constitution and microwave dielectric properties of  $\text{Zn}_3\text{Nb}_2\text{O}_8-\text{TiO}_2$ . *Jpn. J. Appl. Phys.*, 2001, **40**(1–10), 5994–5998.
16. Kim, D.-W., Kim, J.-R., Yoon, S.-H. and Sun Hong, K., Microwave dielectric properties of low fired  $\text{Ba}_5\text{Nb}_4\text{O}_{15}$ . *J. Am. Ceram. Soc.*, 2002, **85**(11), 2759–2762.
17. Wu, M.-C., Huang, K.-T. and Su, W.-F., Microwave dielectric properties of doped  $\text{Zn}_3\text{Nb}_2\text{O}_8$  ceramics sintered below  $950^\circ\text{C}$  and their compatibility with silver electrode. *Mater. Chem. Phys.*, 2006, **98**, 406–409.
18. Petricek, V. and Dusek, M., *Jana 2000, the crystallographic computing system*. Institute of Physics, Praha, Czech Republic, 2000.
19. Kim, D.-W., Hong, K. S., Yoon, C. S. and Kim, C. K., Low temperature sintering and microwave dielectric properties of  $\text{Ba}_5\text{Nb}_4\text{O}_{15}-\text{BaNb}_2\text{O}_6$  mixtures for LTCC applications. *J. Eur. Ceram. Soc.*, 2003, **23**, 2597–2601.
20. Volkov, V. L., Fotiev, A. A., Fedotovskikh, N. G. and Andreikov, E. I., Phase diagram of the vanadium pentoxide–copper vanadium oxide ( $\text{V}_2\text{O}_5-\text{CuV}_2\text{O}_5$ ) and vanadium pentoxide silver systems. *Zh. Fiz. Khim.*, 1974, **48**(6), 1514–1515.
21. Wang, J., Yue, Z., Gui, Z. and Li, L., Low-temperature sintered  $\text{Zn}(\text{Nb}_{1-x}\text{V}_{x/2})_2\text{O}_{6-2.5x}$  microwave dielectric ceramics with high  $Q$  value for LTCC application. *J. Alloy Compd.*, 2005, **392**(1–2), 263–267.
22. Roulland, F., Allainmat, G., Pollet, M. and Marinell, s., Low temperatures sintering of the binary complex perovskite oxides  $x\text{Ba}(\text{zn}_{1/3}\text{Ta}_{2/3})_3 + (1-x)\text{Ba}(\text{Mg}_{1/3}\text{Ta}_{2/3})\text{O}_3$ . *J. Eur. Ceram. Soc.*, 2005, **25**, 2763–2768.